

This is an Open Access document downloaded from ORCA, Cardiff University's institutional repository:<https://orca.cardiff.ac.uk/id/eprint/133445/>

This is the author's version of a work that was submitted to / accepted for publication.

Citation for final published version:

Guo, Junli, Shi, Lianqiang, Pan, Shunqi , Ye, Qinghua, Cheng, Wufeng, Chang, Yang and Chen, Shenliang 2020. Monitoring and evaluation of sand nourishments on an embayed beach exposed to frequent storms in eastern China. *Ocean & Coastal Management* 195 , 105284. 10.1016/j.ocecoaman.2020.105284

Publishers page: <http://dx.doi.org/10.1016/j.ocecoaman.2020.105284>

Please note:

Changes made as a result of publishing processes such as copy-editing, formatting and page numbers may not be reflected in this version. For the definitive version of this publication, please refer to the published source. You are advised to consult the publisher's version if you wish to cite this paper.

This version is being made available in accordance with publisher policies. See <http://orca.cf.ac.uk/policies.html> for usage policies. Copyright and moral rights for publications made available in ORCA are retained by the copyright holders.



1           **Monitoring and evaluation of sand nourishments on an**  
2           **embayed beach exposed to frequent storms in eastern China**

3           Junli Guo<sup>a</sup>, Lianqiang Shi<sup>b</sup>, Shunqi Pan<sup>c</sup>, Qinghua Ye<sup>d</sup>, Wufeng Cheng<sup>a</sup>, Yang Chang<sup>a</sup>,  
4           Shenliang Chen<sup>a,\*</sup>

5           <sup>a</sup> *State Key Laboratory of Estuarine and Coastal Research, East China Normal*  
6           *University, Shanghai 200241, China*

7           <sup>b</sup> *Second Institute of Oceanography, Ministry of Natural Resources of China, Hangzhou*  
8           *310012, China*

9           <sup>c</sup> *Hydro-environmental Research Centre, School of Engineering, Cardiff University,*  
10          *Cardiff CF24 3AA, UK*

11          <sup>d</sup> *Deltares, Delft 2614HV, the Netherlands*

12          \*Corresponding author.

13          *E-mail address: slchen@sklec.ecnu.edu.cn (S. Chen)*

14

15

16

17

18

19

20

21 **Abstract**

22 Beach nourishment is a proved effective protection approach which has been widely  
23 used in recent years. An Argus video monitoring system has been set up to monitor  
24 morphological changes and effects of continuous nourishments at Dongsha beach, an  
25 embayed beach in Zhoushan Archipelago, eastern China. Video-derived shorelines  
26 along with their morphological parameters, such as dry beach width, dry beach area,  
27 beach orientation and unit width volume were analyzed during the monitoring period  
28 from June 2016 to July 2017. Analysis of video monitoring data shows that shorelines  
29 retreated during autumn and winter when storms were intensive, while advanced in  
30 spring and summer, with a lot of bulges occurred after nourishment projects. Abrupt  
31 variations in the beach orientation were always followed by gradual recoveries to the  
32 average beach orientation, while continuous counter-clockwise rotation occurred after  
33 March, 2017 when storm events were sparse. Comparing the different beach responses  
34 to individual storm events, we found that small-scale and short-interval sand  
35 nourishment implemented timely after storms can compensate for sediment loss more  
36 effectively on this beach. This study can provide a reference for local beach  
37 management.

38 **Keywords:** Argus video monitoring; beach nourishment; storm erosion; occurrence  
39 time of nourishment; beach management

40

41

## 42 **1. Introduction**

43 Due to the global climate change with sea level rise and more frequent and severe  
44 storms, serious beach erosion is observed all over the world ([Castelle et al., 2007](#);  
45 [Houston and Dean, 2014](#); [Qi et al., 2010](#); [Scott et al., 2016](#); [Smith et al., 2014](#)). At least  
46 70% of sandy beaches experienced widespread erosion around the world ([Bird, 1985](#)),  
47 and approximately 50% of sandy coasts were regressed in erosion in China ([Third  
48 Institute of Oceanography, 2010](#)). Under this circumstance, there are growing numbers  
49 of beach protection or restoration projects in China, particularly in the tourism hotspots,  
50 to meet increasing public requirements ([Kuang et al., 2011](#)).

51 The common approach adopted in the past to protect or restore beaches is the hard  
52 engineering based ([Cai et al., 2011](#); [Pan, 2011](#)). Although hard engineering, such as  
53 artificial coastal structures, can effectively mitigate shoreline retreat caused by storms,  
54 it may have negative impacts on its adjacent beach ([Hamm et al., 2002](#)). For decades,  
55 beach nourishment has become a preferred method to protect beaches in developed  
56 countries ([Castelle et al., 2009](#); [Cooke et al., 2012](#); [Hamm et al., 2002](#); [Hanson et al.,  
57 2002](#); [Pan, 2011](#)), which has also been frequently applied in China in recent years ([Luo  
58 et al., 2016](#)).

59 However, beach nourishments can often cause large-scale nearshore disturbances  
60 that affect the balance of alongshore and cross-shore sediment transport ([Dean, 1983](#)).  
61 Under natural conditions, storm-eroded sandy beaches may recover gradually over  
62 seasons to a decade timescale ([Harley et al., 2015](#); [Scott et al., 2016](#)), while the beach

63 processes with nourishment disturbance vary significantly (Elko et al., 2005; Seymour  
64 et al., 2005). Previous studies focused on nourishments with regular frequency and  
65 fixed implement timing in European countries (Hanson et al., 2002), the USA (Leonard  
66 et al., 1989) and Australia (Cooke et al., 2012). However, the beach protection approach  
67 at Zhoushan Archipelago in China is different due to frequent occurrence of storms. To  
68 prevent the severe storm erosion and maintain the recreational beach, small-scale and  
69 irregular nourishments have been frequently implemented and the occurrence time of  
70 those nourishments is often close to the storm period. Up to the present, beach  
71 morphodynamic evolution involved with this beach protection approach remains  
72 unclear.

73       Understanding the self-adjustment of beaches after nourishments is important for  
74 management (Elko and Wang, 2007), while there is always no regular monitoring of  
75 changes in beaches after nourishments (Chiva et al., 2018; Leonard et al., 1989; Stauble,  
76 1988). Video monitoring systems are proved to be adequate in detecting and quantifying  
77 spatial and temporal beach responses (Archetti and Romagnoli, 2011). Especially,  
78 Argus system has been widely used in beach morphodynamic research in recent  
79 decades (Angnuureng et al., 2017; Balouin et al., 2013; Karunaratna et al., 2014).

80       Nourishment can be further evaluated based on the continuous imagery data  
81 obtained by video monitoring. Beach morphological variations and longevity of  
82 borrowed sediments are criteria to evaluate the effectiveness of beach nourishment (Liu  
83 et al., 2019; Psuty and Moreira, 1992). Factors affecting the beach nourishment

84 longevity include parameters of nourishment projects and physical characteristics of  
85 beaches. The former mainly includes sediment characteristics, such as grain size  
86 distribution (Chiva et al., 2018; Pranzini et al., 2018; Stauble, 2007), mineral  
87 component (Pagán et al., 2018), volume scale (Basterretxea et al., 2007; Stauble, 2007)  
88 and spatial location (Karambas and Samaras, 2014) of borrowed sediments. The latter  
89 consists of wave/wind regimes (Karambas and Samaras, 2014) and the native  
90 morphological characteristics of beaches (Liu et al., 2019). Different combinations of  
91 those factors will result in different nourishment impacts on the beach.

92 In this study, we selected Dongsha beach, a 1.5 km-long embayed sandy beach in  
93 Zhoushan Archipelago of China, to observe its morphodynamics and evaluate the  
94 effectiveness of nourishments. An Argus video monitoring system was used to record  
95 variability of beach morphology. Beach morphological parameters including: dry beach  
96 width, shoreline displacement, dry beach area, beach orientation and rotation, and unit  
97 width volumetric change for more than a year were analyzed using Argus imagery data.  
98 Beach responses to individual storm events in five different cases were also revealed in  
99 detail. Based on morphological analysis, the evaluation of nourishment effectiveness  
100 and factors affecting nourishment longevity were discussed. Beach nourishment  
101 implications were proposed for further beach management.

## 102 **2. Materials and methods**

### 103 **2.1. Study area**

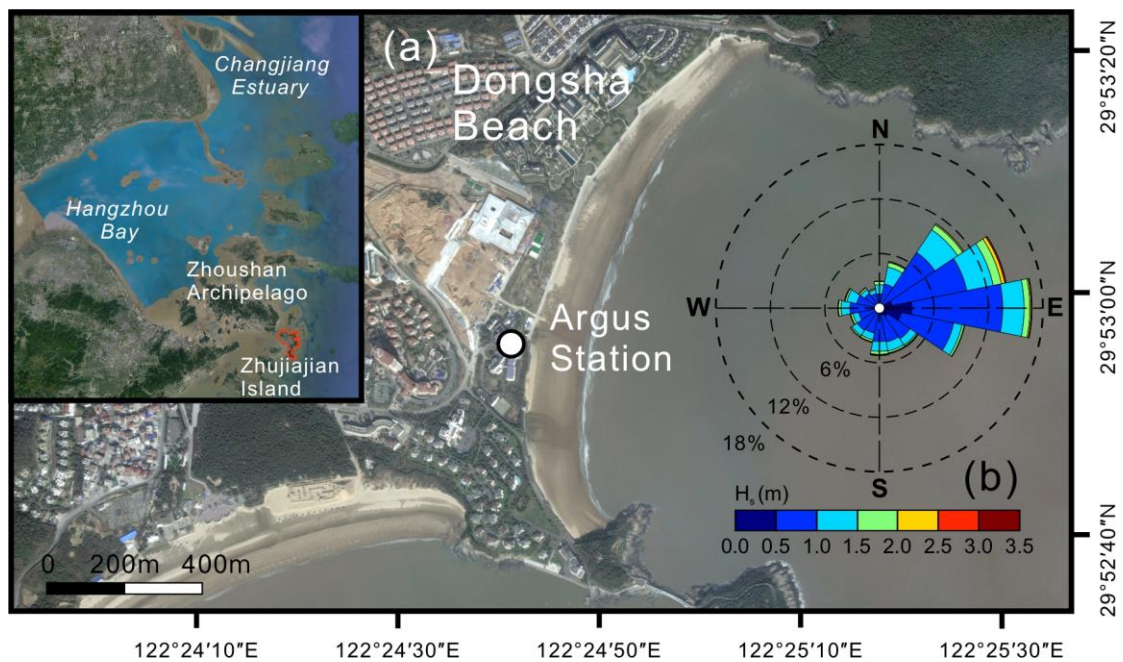
104 Approximately 50% of sandy coasts were regressed in erosion in China over past

105 several decades (Third Institute of Oceanography, 2010). Thus, a large amount of beach  
106 nourishment projects have been accomplished along China's coast since the 1990s (Cai  
107 et al., 2011; Kuang et al., 2019; Luo et al., 2016). Zhoushan Archipelago is a popular  
108 tourism destination with more than 30 embayed beaches (Xia, 2014), at a location  
109 connecting the Hangzhou Bay and the East China Sea. Typhoon is a common coastal  
110 hazard affecting the Archipelago with a frequency of 6 times a year on average (Lu,  
111 2010), which has a significant impact on beach morphology and even threatens the  
112 tourism. Dongsha beach was selected as the study area, which is located at Zhujiajian  
113 Island in Zhoushan Archipelago (Fig. 1a). It is an embayed beach bounded by headlands  
114 with a total length of about 1500 m and is a typical tourism beach. To monitor the  
115 detailed evolution of the beach, an Argus video monitoring system with six cameras  
116 (Fig. 1a and Fig. 2) was installed on 2015.

117 Slope of Dongsha beach varies alongshore, with measured values between 2.9%  
118 and 3.5%. The steepest transects were found at the northern beach and the southern  
119 transects were the flattest (calculated according to Guo et al., 2018). The median grain  
120 size ( $D_{50}$ ) of sediments on the beach range between 0.15 mm and 0.38 mm (fine sand).  
121 The beach sediments mainly come from the erosion of coastal rocks eroded by the wind  
122 and wave (Cheng et al., 2014). There is no direct river input around the Dongsha beach  
123 (Xia, 2014). Fine-grained sediments are rich in the adjacent sea area of the Zhoushan  
124 Archipelago due to the coastal current induced southward transportation of sediments  
125 from the Yangtze River (Hu et al., 2009; Li et al., 2018), and there is a sand-mud

126 transition located on the 5 m of isobath in the adjacent sea area of Dongsha beach (Cheng  
 127 et al., 2014). There were sand dunes in the backshore of the beach, while the  
 128 construction of the seawall has broken the balance of cross-shore sediment transport on  
 129 the beach (Cheng et al., 2014; Guo et al., 2018), further resulting in the disappearance  
 130 of dunes.

131 Tidal data provided by Shenjiamen tidal gauge station (29.93°N,122.3°E) shows  
 132 that tides are mainly semi-diurnal and the mean tidal range is 2.6 m. Wave  
 133 measurements were simultaneously obtained hourly by a wave buoy (29.8°N,122.5°E)  
 134 located about 12 km offshore in 20 m depth. The offshore wave climate is characterized  
 135 by low to moderate wave energy (mean  $H_{sig} \approx 0.82$  m,  $T_{peak} \approx 6.2$  s). Fig. 1b indicates the  
 136 overall wave rose for the buoy. The prevailing waves come from the East, and direction  
 137 of high waves range from Northeast to Southeast with a maximum significant wave  
 138 height of 3.1 m.



139

140 **Fig. 1.** Sketch of study area (a) and wave rose of the study area (b), in which  $H_s$  is the  
141 significant wave height. The satellite images obtained from Google Earth.

## 142 **2.2. Beach nourishment**

143 Seawall construction and the intensive storm events resulted in long-term erosion  
144 of Dongsha beach (Guo et al., 2018). To prevent storm erosion and widen recreational  
145 beach, beach nourishment projects were initiated in September 2016. Nourishment with  
146 irregular time, small scale and limited spatial distribution is the main beach  
147 maintenance pattern implemented on Dongsha beach, which is also common in China.  
148 The beach management department carried out 10 beach nourishment projects during  
149 2016 and 2017 (Table 1, Fig. 2) with a total sand volume of  $\sim 52,000 \text{ m}^3$ . The borrowed  
150 sediments were mainly placed in the area between transect 16 and transect 28, and the  
151 alongshore sand placement was limited in the area between transect 10 and transect 29  
152 (Fig. 2) due to the restraints of transportation condition on the beach. All the  
153 nourishments have the same operations and materials which has the similar  
154 characteristics with the native sediments.

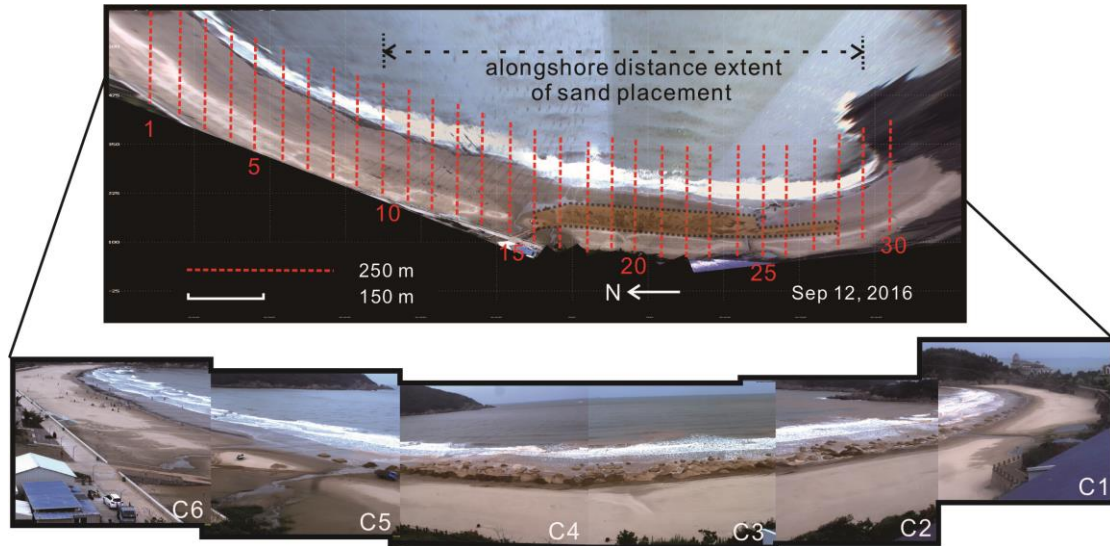
155 **Table 1**

156 Information of beach nourishments on Dongsha beach.

Nourishment	Time span	Sand volume ( $\text{m}^3$ )	Beach position
N1	9 Sep, 2016 - 13 Sep, 2016	$\sim 10000$	Southern
N2	24 Sep, 2016	$\sim 1000$	Southern
N3	29 Sep, 2016 - 30 Sep, 2016	$\sim 2000$	Southern
N4	4 Oct, 2016 - 8 Oct, 2016	$\sim 5000$	Southern
N5	31 Oct, 2016 - 10 Nov, 2016	$\sim 10000$	Southern & Central
N6	5 Jan, 2017 - 13 Jan, 2017	$\sim 10000$	Southern

N7	18 Jan, 2017 - 19 Jan,2017	~2000	Southern
N8	31 Jan, 2017 - 8 Feb, 2017	~10000	Southern
N9	18 Feb, 2017	~1000	Southern
N10	18 May, 2017	~1000	Southern

157



158

159 **Fig. 2.** Planview of Dongsha beach merged by snap images of six cameras (C1-C6)

160 during N1 period (yellow shadow area shows the sand placement). 30 transects (red

161 dotted lines) were set every 50 m on the beach surface from north to south (from  $y =$

162 900 to  $y = -550$ ), northward coordinates alongshore and eastward coordinates cross-

163 shore with respect to Argus station are positive.

### 164 2.3. Identification of storm events

165 According to the method proposed by [Boccotti \(2000\)](#), storm events were

166 identified when the significant wave height is greater than 1.5 times the annual average

167 (0.82 m in this research) with duration  $\geq 12$  hours, which was based on the *in situ* data

168 obtained by buoy. 19 storm events (S1-S19) were extracted during the study period

169 from June 1, 2016 to July 1, 2017 ([Fig. 3](#)). Then, the wave energy storm peak  $E$  ( $m^2s$ )

170 was calculated as:

$$171 \quad E = H_{max}^2 \cdot T_p \quad (1)$$

172 where  $H_{max}$  represents the maximum storm significant wave height, and  $T_p$  is the wave  
173 period at the storm peak (Archetti et al., 2016; Harley et al., 2014; Senechal et al., 2015).

174 The storm power index  $P_s$  ( $m^2h$ ) (Dolan and Davis, 1992) was also calculated:

$$175 \quad P_s = H_{max}^2 \cdot D \quad (2)$$

176 where  $D$  is the duration of “storm conditions” in hours.

#### 177 **2.4. Beach morphological variation processing**

178 Real-time and continuous imagery was extracted from the Argus video monitoring  
179 system, with a frequency of 2 Hz in 10-min bursts every daylight half hour, including  
180 Snapshot images, Timex images, and Variance images with a resolution of 2448×2048  
181 pixels. To validate the accuracy of the beach morphology obtained by the Argus system,  
182 a field survey was carried out at Dongsha beach on May 4, 2016 using RTK GPS, and  
183 a total of 41 ground control points were measured. The results showed that the average  
184 vertical error is 0.145 m, and more details were introduced by Guo et al.(2019).

185 The images from June 2016 to July 2017 were selected from the image dataset for  
186 beach nourishment evolution analysis. All images of the months when the storm events  
187 and sand nourishments were concentrated (September 1, 2016 - February 28, 2017)  
188 were selected, and only partial images of the rest months were selected. Based on the  
189 merged images of Argus cameras, 30 transects were set every 50 m on the beach from  
190 north to south (from  $y = 900$  to  $y = -550$ , Fig. 2). Then unit width volume change and

191 shoreline position of each transect were calculated in Argus Intertidal Bathymetry  
192 Mapper module (Aarninkhof et al., 2003).

193 Dry beach width ( $DBW$ ) can be calculated by shoreline position (Harley et al.,  
194 2014) as follows:

$$195 \quad DBW_i = X_{shoreline,i} - X_{seawall,i} \quad (3)$$

196 where  $X_{shoreline,i}$  is the position of shoreline obtained from Argus at transect  $i$ , and  
197  $X_{seawall,i}$  represents the position of the seawall at transect  $i$ .

198 The alongshore-averaged dry beach width ( $\overline{DBW}$ , Harley et al., 2014) for the  
199 beach was also calculated:

$$200 \quad \overline{DBW} = \frac{1}{N} \sum_{i=1}^N DBW_i \quad (5)$$

201 where the number of transects  $N$  is 30.

202 Dry beach area ( $DBA$ ) is an important parameter for the beach management, which  
203 determines the space available for beach tourists.  $DBA$  can be approximately calculated  
204 according to Harley et al. (2014) as:

$$205 \quad DBA \approx \Delta S \sum_{i=1}^N DBW_i \quad (6)$$

206 where  $\Delta S$  represents alongshore spacing between transects ( $\Delta S=50$  m).

207 Changes in shoreline position are often in response to sediment supply, sea level  
208 rise, climate change, and human intervention (Karunaratna et al., 2018). In order to  
209 describe the response of Dongsha beach over the study period, the mean distance  $\Delta x$   
210 (distance between shoreline of Jun 1, 2016 and later days in cross-shore direction during  
211 the study period) was calculated according to Archetti et al. (2016) as:

212 
$$\Delta x = \frac{\sum_i d_i}{n} \quad (7)$$

213 where  $i$  is the transect ( $i=1-30$ ),  $d_i$  is the distance between shorelines in cross-shore  
214 direction at each transect and  $n$  is the transect number ( $n=30$ . The previous field  
215 investigation in Dongsha beach showed that 30 transects could represent the whole  
216 beach in this study).

217 Shoreline variability is additionally influenced by beach rotation on embayed  
218 beaches (Short and Masselink, 1999), and beach rotation is a key process for  
219 understanding the morphodynamic of embayed beaches (Ojeda and Guillén, 2008).  
220 Beach orientation and rotation were calculated according to Ojeda and Guillén (2008)  
221 in this study, positive (negative) rotation value corresponds to a more clockwise  
222 (counter-clockwise) orientation. A degree change in beach orientation means a 26 m  
223 shoreline change of the two extremities in Dongsha beach.

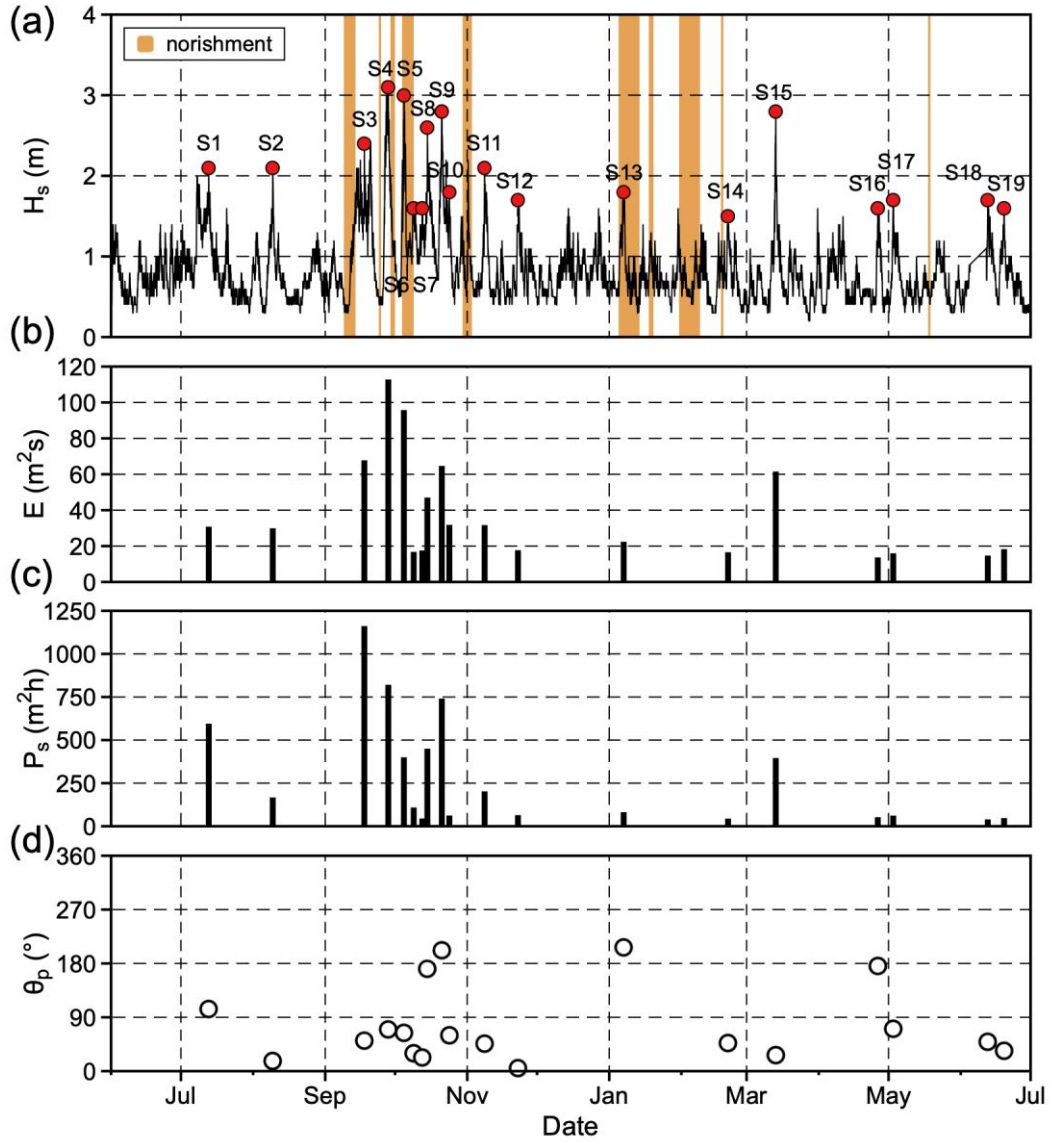
224 Based on the morphological variation of the beach, the longevity of each  
225 nourishment could be calculated. The longevity in this study represents the lasting  
226 duration of borrowed sediments, it is the time duration when the mean unit width  
227 volume is larger than that before the nourishment.

## 228 **3. Results**

### 229 **3.1. Storm characteristics**

230 A total of 19 storm events (S1-S19) were extracted during the study period from  
231 June 1, 2016 to July 1, 2017 (Fig. 3).  $H_{max}$  and  $T_p$ ,  $D$ , storm direction  $\theta_p$  (wave direction  
232 at the storm peak with respect to north),  $E$  and  $P_s$  were summarized for all the storm

233 events. The strongest storm event (S3) occurred in September 2016 with a  $P_s$  of 1157.76  
234  $\text{m}^2\text{h}$ , which is identified as significant severity ( $P_s > 500 \text{ m}^2\text{h}$ ) according to [Mendoza et](#)  
235 [al. \(2011\)](#). Overall, four storm events over the study period were categorized as  
236 significant, and three as moderate ( $251 < P_s \leq 500 \text{ m}^2\text{h}$ ), with the remaining 12 events  
237 recognized as calm ( $P_s \leq 250 \text{ m}^2\text{h}$ ) ([Fig. 3c](#)). As shown in [Fig. 3](#), storm events were  
238 predominantly intensive in autumn (September - November), with a minority of calm  
239 events occurring within the winter months (December - February). It can be seen that  
240 peak direction of these storm events mainly distribute between north and east, with a  
241 small number of storm events having a south direction.



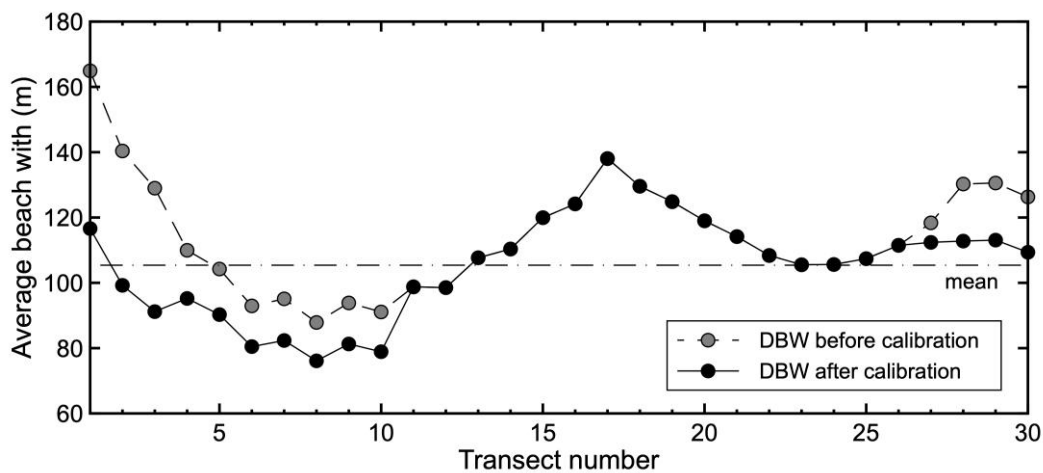
242

243 **Fig. 3.** Significant wave height ( $H_s$ ) over the study period (a), storm energy  $E$  (b), storm  
 244 power index  $P_s$  (c) and the peak direction  $\theta_p$  (d) of each storm event. Red circles  
 245 represent the peak significant wave heights during storm events, while the dark yellow  
 246 shadow areas show the time span of each nourishment project.

247 **3.2. Morphological variation of Dongsha beach**

248 Averaged  $DBW$  at each transect was quantified for the beach over the study period  
 249 as shown in Fig. 4. Since some transects (1-10 and 27-30) are not perpendicular to the

250 shoreline (Fig.2), calibrations of *DBW* at those transects were done (Fig. 4). Generally,  
 251 the northern part of the beach had the narrowest *DBW* while the middle part of the beach  
 252 had the widest *DBW* over the study period. *DBW* of Dongsha beach ranges from 76 m  
 253 (transect 8) to 138 m (transect 17). It is worth noting that the beach tourism facilities  
 254 are located on the area with larger *DBW* than the average (area between transect 13 and  
 255 transect 23), which is also the tourist-dense area.



256

257 **Fig. 4.** Averaged dry beach width at each transect over the study period.

258 The majority of  $\Delta x$  values range generally between -25 and 20 m over the 13  
 259 months (Fig. 5a). There were a few higher positive values (from 20 to 49 m) came after  
 260 nourishments, and a few lower values occurred commonly in the storm-intensive period.  
 261 The largest shoreline retreat (-42.6 m) came after the last storm event during the storm-  
 262 intensive period, while the largest advance (49 m) occurred in the latter part of study  
 263 period without storm event. Temporal distribution of  $\Delta x$  values over the whole study  
 264 period suggests that shorelines retreated during autumn and winter while advanced in  
 265 spring and summer. It is worth noting that a lot of peak values occurred after

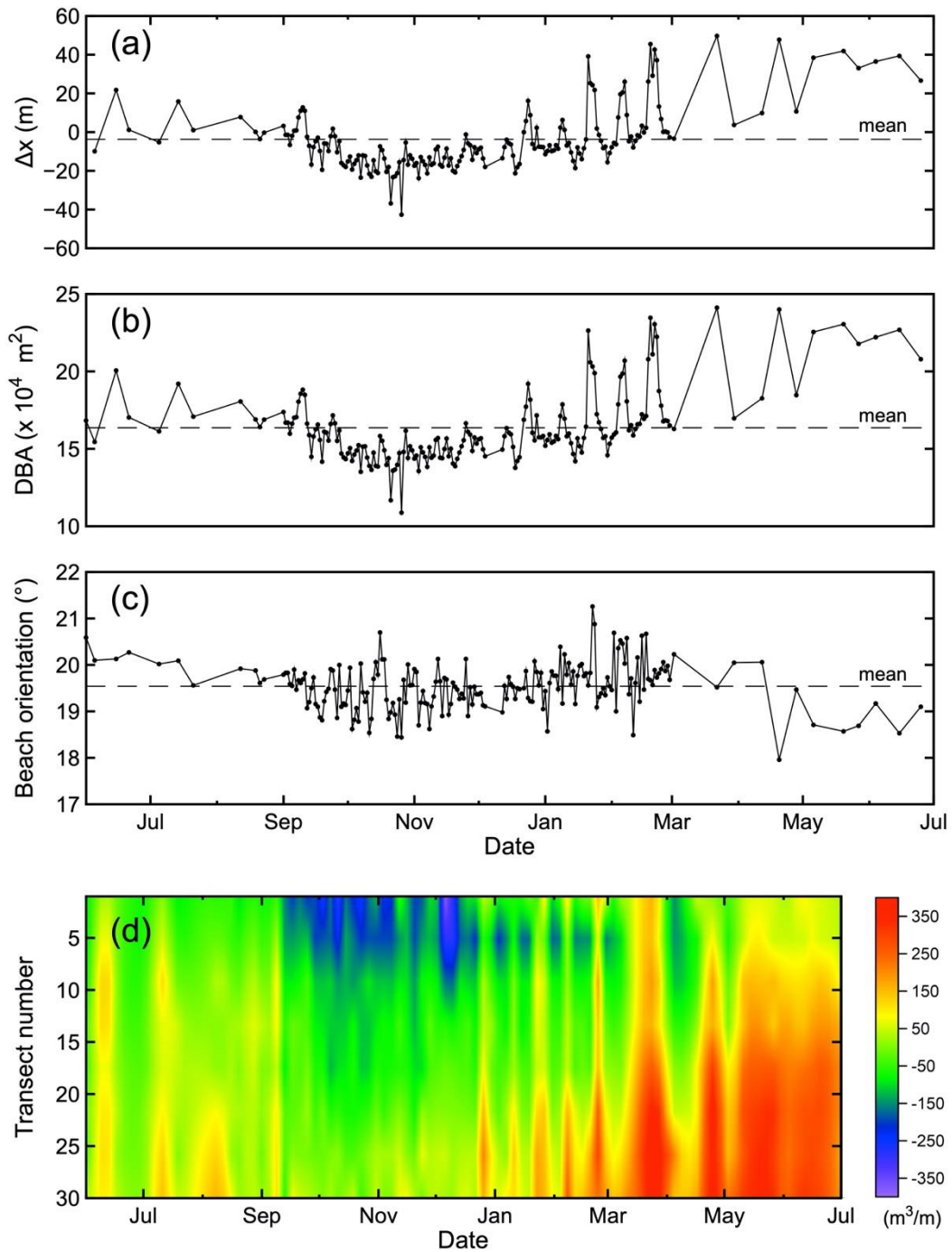
266 nourishment projects.

267 Temporal evolution of *DBA* has the similar pattern with  $\Delta x$  (Fig. 5b). *DBA* values  
268 range from 108,848 m<sup>2</sup> to 241,216 m<sup>2</sup>, with an average of 163,635 m<sup>2</sup> over the whole  
269 study period. Dry beach area values smaller than the average also mainly occurred in  
270 autumn and winter when storm events were intensive.

271 The variation pattern of beach orientation is shown temporally in Fig. 5c.  
272 Generally, abrupt variations in the beach orientation (caused by storm events or  
273 nourishments) were always followed by gradual recoveries to 19.5° (the average beach  
274 orientation). Beach rotation varied between a minimum value of -2.63° and a maximum  
275 of 0.67°. Clear rotation was identified as counter-clockwise after March, 2017 when  
276 storm events were sparse.

277 The unit width volumetric change highly depends on the alongshore position with  
278 an average of -60.4 m<sup>3</sup>/m and various patterns are present at the northern (transect 1-  
279 10), middle (transect 11-20) and southern (transect 21-30) beach (Fig. 5d). It is shown  
280 that the largest positive volumetric change occurred on transect 29 (488 m<sup>3</sup>/m) and the  
281 largest negative on transect 9 (-460 m<sup>3</sup>/m). The overall variation of unit width volume  
282 indicates a transition from erosion in the north to accretion in the south under calm  
283 conditions, while the erosion of northern beach is more severe than the southern beach  
284 after storm events. Averaged unit width volumetric changes are 14.4 m<sup>3</sup>/m, -59.71 m<sup>3</sup>/m,  
285 -0.23 m<sup>3</sup>/m, and 139.97 m<sup>3</sup>/m in summer, autumn, winter and spring, respectively,  
286 suggesting an seasonal variation pattern: slight accretion-severe erosion-slight erosion-

287 strong accretion. Most of the obvious accretion (erosion) peak values commonly  
288 correspond to nourishments (storm events). In addition, the borrowed sediments were  
289 mainly placed between transect 16-28 ([Fig. 2](#)), while the distribution of obvious  
290 accretion peaks commonly ranged from transect 15-30, indicating the nourishment  
291 impact on beach.



292

293 **Fig. 5.** Distribution of shoreline displacement ( $\Delta x$ ) (a), dry beach area (DBA) (b), beach  
 294 orientation (c) and unit width volumetric change ( $\Delta V$ ) (d) of Dongsha beach over the  
 295 study period.

296 **3.3. Beach responses to individual storm events**

297 There were 19 storm events over the study period with various impacts on  
298 Dongsha beach. Table 2 shows the  $\Delta x$ , change in dry beach area ( $\Delta DBA$ ), unit width  
299 volumetric change ( $\Delta V$ ), and beach rotation during each storm event. Since most of the  
300 storm events occurred along with beach nourishments, beach responses to individual  
301 storm events are different and complex. According to the relationship between the  
302 occurrence time of the storm events and nourishments, we divided beach responses (to  
303 individual storm events) into five cases (Table 2). In Table 2, we chose the nourishment  
304 event with the nearest occurrence time in depicting the occurrence time of each storm  
305 event. E.g., if S3 occurred in 1 day after N1 and 4 days before N2, then the occurrence  
306 time of S3 in Table 2 would be recognized as 1 day after N1.

#### 307 ***Case1: Without nourishment***

308 Case1 includes the storm events occurred before the beginning of nourishment  
309 projects (S1 and S2). The two storm events with moderate  $H_s$  in Case1 produced none  
310 erosion but advances in shoreline (Table 2). In the meanwhile, beach rotation is not  
311 significant in this case.

#### 312 ***Case2: Nourishment occurred before storm event***

313 Case2 consists of the storm events occurred after nourishments (S3, S4, S6, S7,  
314 S8, S9 S12, S14 and S15). S3 has the longest duration with the highest  $P_s$  of 1157.76  
315  $m^2h$ , but did not cause the most severe erosion. While S4 with the second higher  $P_s$ ,  
316 induced the severest beach erosion of 79.16  $m^3/m$  and 15.83 m retreat in shoreline (Fig.  
317 3 and Table 2). Different beach responses to S3, S4, S9 and S14 may correlate with

318 sand volume scale of nourishment projects. S3 and S9 occurred after two large sand  
319 nourishments ( $\sim 10000 \text{ m}^3$  and  $\sim 5000 \text{ m}^3$ , respectively), while S4 and S14 occurred after  
320 two small sand nourishments ( $\sim 1000 \text{ m}^3$ ). Although nourishments implemented before  
321 storm events can compensate for the sediment loss, the beach still lost a lot of sediments  
322 after those four storm events. However, storm events identified as calm (S6, S7, S8,  
323 S12, S15) occurred after nourishments did not cause erosion. The results of this case  
324 show that nourishments before storm events can be effective only when the storm  
325 energy is low. Beach rotation varied significantly in this case without regular pattern.  
326 In the meanwhile, consecutive storm events did not show cumulative erosion in this  
327 case.

#### 328 ***Case3: Nourishment occurred at the same time with storm event***

329 There were two pairs of storm events and nourishments happened at the same time:  
330 N5 and S11, N6 and S13. The two storm events in this case showed no erosion but  
331 accretion with the same volume ( $\sim 5000 \text{ m}^3$ ) nourishments (Table 2). The different  $\Delta x$   
332 corresponds well to the different storm energy in this case: the higher the storm energy  
333 is, the larger the shoreline displacement is.

#### 334 ***Case4: Nourishment occurred after storm event***

335 Three storm events (S5, S10, S17) in this case did not cause any erosion (Table 2).  
336 Especially, S5 with a  $H_{max}$  of 3 m did not cause shoreline retreat, which might due to  
337 the compensation of N5. The result shows that nourishments in this case compensated  
338 the sediment loss effectively.

339 ***Case5: Long interval between storm event and nourishment***

340 S18 and S19 occurred at the end of study period. S18 made no erosion but a  $0.64^\circ$   
341 counter-clockwise beach rotation, while S19 caused a 12.75 m retreat in shoreline with  
342 a  $0.57^\circ$  clockwise beach rotation. Although the two storm events in this case had the  
343 similar  $E$  and  $P_s$  (Fig. 3), the impacts vary. Furthermore, the calm storm S19 caused  
344 significant erosion of the beach, and its erosion degree even exceeded S3, S9 and S14,  
345 indicating that the borrowing sediments before the storm event has compensated for the  
346 beach loss during those storm events. When there is no borrowed sediment to make up  
347 for the loss, a calm storm event like S19 can cause a shoreline retreat of more than 10  
348 m.

349 Comparing the above five cases, we could get the results that the storm erosion  
350 can be fully compensated by sand nourishment no matter when the nourishment project  
351 occurred for storm events identified as calm ( $P_s \leq 250 \text{ m}^2\text{h}$ ). Regarding moderate ( $251 <$   
352  $P_s \leq 500 \text{ m}^2\text{h}$ ) and significant ( $P_s > 500 \text{ m}^2\text{h}$ ) severity storm events, borrowing  
353 sediments timely after the storm event is the most effective way to maintain Dongsha  
354 beach. Although the beach did not show significant erosion when the storm events and  
355 nourishments occurred simultaneously, the nourishment effect was not so significant as  
356 in Case 4. Nourishments in Case1, Case2, Case3 and Case4 all have compensated for  
357 the storm erosion. However, the sediment loss caused by storm erosion cannot be  
358 compensated in Case5 due to the long interval between storm events and nourishments,  
359 which made the calm storm (e.g. S19) cause severe erosion.

360 **Table 2**  
 361 Morphological variations of Dongsha beach after individual storm events during the study period.

Case	Storm	$H_{max}$ (m)	Occurrence Time (refer to Fig. 3)	$\Delta V$ (m <sup>3</sup> /m)	$\Delta x$ (m)	$\Delta DBA$ (m <sup>2</sup> )	Rotation (°)	Recovery period (day)
1	S1	2.10	without nourishment	105.16	21.03	30704	0.07	/
1	S2	2.10	without nourishment	33.80	6.76	9862	0.37	/
2	S3	2.40	1 day after N1	-36.85	-7.37	-10839	0.42	no recovery
2	S4	3.10	2 days after N2	-79.16	-15.83	-23113	-0.33	no recovery
2	S6	1.60	1 day after N4	9.66	1.93	3812	-1.49	/
2	S7	1.60	4 days after N4	34.79	6.96	8455	1.16	/
2	S8	2.60	6 days after N4	26.28	5.26	7704	0.42	/
2	S9	2.80	14 days after N4	-37.82	-7.56	-9455	-1.66	no recovery
2	S12	1.70	7 days after N5	41.53	8.31	11988	-0.19	/
2	S14	1.50	2 days after N9	-41.78	-8.36	-12327	0.06	32
2	S15	2.80	21 days after N9	265.49	53.10	78313	-0.71	/
3	S11	2.10	at the same time with N5	3.65	0.73	909	0.14	/
3	S13	1.80	at the same time with N6	58.82	11.76	16375	0.63	/
4	S5	3.00	1 day before N4	2.98	0.60	1928	-1.17	/
4	S10	1.80	7 days before N5	36.71	7.34	10651	0.33	>13
4	S17	1.7	14 days before N10	138.85	27.77	40807	-0.76	/
5	S16	1.6	60 days after N9	-185.52	-37.1	-55230	1.51	24
5	S18	1.60	27 days after N10	14.54	2.91	4811	-0.64	/
5	S19	1.70	31 days after N10	-63.75	-12.75	-19046	0.57	>7

362

## 363 4. Discussion

### 364 4.1. Evaluation of beach nourishments

365 The effectiveness of sand nourishments in this study has been evaluated in terms  
366 of their abilities to meet the project goals, which were to prevent storm erosion and  
367 widen the recreational beach. As for preventing storm erosion, 12 storm events with  
368 none erosion and 3 storm events recovered within several days were observed (Table  
369 2). However, seawall constructed on the beach and the intensive storm events resulted  
370 in long-term erosion. Guo et al. (2018) found that Dongsha beach didn't recover from  
371 a storm event during 2014 and 2015 without sand nourishment, suggesting that the  
372 nourishment projects in this study are successful in preventing storm erosion. In terms  
373 of widening the recreational beach, all the nourishment projects recorded increases in  
374  $\overline{DBW}$  and  $DBA$ . The maximum increases in  $\overline{DBW}$  and  $DBA$  observed over the 10  
375 nourishment periods are 50.18 m and 74755 m<sup>2</sup>, respectively (Table 3). The relatively  
376 short duration of this study limited the assessment of longer-term benefits of the  
377 nourishments, the results only suggest that nourishments on Dongsha beach were  
378 successful in achieving these two goals over a year video monitoring.

379 Although nourishment on this beach have met the project goal, beach  
380 nourishments can often cause large-scale nearshore disturbances that affect the balance  
381 of alongshore and cross-shore sediment transport (Dean, 1983). In general, the sediment  
382 transport on the beach without human intervention is mainly controlled by the  
383 hydrodynamic processes (Wiggins et al., 2019) and beach characteristics (Oliveira et al.,  
384 2017). Sediment transport on the beach can be more complex with human activities

385 (Duvat et al., 2019; Luo et al., 2016). Cheng et al.(2014) found that significant erosion  
386 in summer and accretion in winter were the main seasonal variation pattern of Dongsha  
387 beach without nourishment, while the beach accreted in summer months with  
388 nourishment in this study. In addition, the distribution of erosion/ accretion on Dongsha  
389 beach also varies with and without nourishments. The beach used to be eroded in the  
390 southern beach (Cheng et al., 2014), while significant accretion can be seen on the  
391 southern beach with nourishment. The change of seasonal variation pattern and  
392 erosion/accretion distribution on this beach may be related to the nourishment impacts,  
393 and further study on sediment transport needs the support of sediment information.

394 Besides, longevities of the borrowed sediments in this study can only be  
395 considered short compared with beach nourishments in Europe countries (Hamm et al.,  
396 2002; Hanson et al., 2002) and the USA (Leonard et al., 1989). Generally, the larger  
397 scale of volume produced the better effectiveness on both morphological variation and  
398 longevity of borrowed sediments (Table 3). In the meanwhile, beach nourishment with  
399 the largest volume did not always cause the largest increase in  $\overline{DBW}/DBA$  and the  
400 longest longevity due to the intensive storm events. For example, N1 with about 10000  
401 m<sup>3</sup> borrowed sediments but only has a 3-day longevity. Although the borrowed  
402 sediments limited in the tourist-dense area (Fig. 6) could meet the recreational need,  
403 counter-clockwise rotation was identified after 9 nourishment projects. The advances  
404 in southern shoreline resulting from the limited sand placement of borrowed sediments  
405 might have contributed to the counter-clockwise rotation in this study. Long-term

406 erosion rates and its spatial gradient is a design guide for the beach nourishment project  
 407 (Kaczkowski et al., 2018), which the spatial location of borrowed sediments should  
 408 depend on. Limited alongshore position of sand placement and the implement timing  
 409 when storm events were intensive are the main causes of those inefficiencies in the  
 410 nourishments in this study.

411 Table 3

412 Beach nourishment longevity and morphological variations of Dongsha beach.

Nourishment	Sand volume (m <sup>3</sup> )	Longevity (days)	$\Delta\overline{DBW}_{max}$ (m)	$\Delta DBA_{max}$ (m <sup>2</sup> )	Beach rotation(°)
N1	~10000	3	5.20	7631	-0.18
N2	~1000	1	3.83	5551	-1.06
N3	~2000	2	3.32	3484	-0.47
N4	~5000	7	7.31	10198	0.09
N5	~10000	59	32.96	47496	-1.39
N6	~10000	8	16.07	24680	-0.27
N7	~2000	11	50.18	74755	-0.26
N8	~10000	18	41.56	61124	-0.98
N9	~1000	7	43.25	63539	-0.61
N10	~1000	3	3.45	5010	-0.15

413 Note:  $\Delta\overline{DBW}_{max}$  is the max change in  $\overline{DBW}$ ;  $\Delta DBA_{max}$  is the max change in  $DBA$ .

414



415

416 **Fig.6.** A snap image taken by the Argus video monitoring system of sand being placed  
417 on the beach (Image date: 12/09/2016 08:00 GMT).

#### 418 **4.2. Factors affecting nourishment longevity**

419 The majority of nourishment projects have a longevity of several years in USA  
420 (Leonard et al., 1989) and Europe countries (Hamm et al., 2002; Hanson et al., 2002).  
421 However, in this study, the longevity of borrowed sediments can only last for several  
422 days to tens of days (Table 3), which correlates well with the wave regime of the study  
423 area. Frequent storms with high significant wave heights make the sediments difficult  
424 to preserve (Table 2).

425 Besides, characteristic of the borrowed sediment can influence the longevity. The  
426 larger volume scale of the borrowed sediments can often causes the longer nourishment  
427 longevity (Cooke et al., 2012; Hamm et al., 2002; Hanson et al., 2002; Leonard et al.,  
428 1989), and the different beach responses to individual storm events in Case2 showed  
429 the similar result. Previous studies also showed that grain size distribution (Chiva et al.,  
430 2018; Pranzini et al., 2018; Stauble, 2007), mineral component (Pagán et al., 2018) and

431 spatial location (Karambas and Samaras, 2014) can affect the nourishment longevity,  
432 which could not be obtained in this study due to the data limitation.

433 It is worth noting that different occurrence time of nourishments is also a  
434 significant factor affecting the longevity. Generally, nourishments occurred timely after  
435 storm events have longer longevity in this study (Table 3). Storm events with high  
436 significant wave heights can take away a great number of sediments on the beach (Coco  
437 et al., 2014; Harley et al., 2014; Qi et al., 2010; Scott et al., 2016; Senechal et al., 2015),  
438 and borrowed sediments might lose more easily than the native sediments during storm  
439 events (Seymour et al., 2005). Nourishments implemented timely after storm events  
440 can not only avoid strong hydrodynamic conditions, but also quickly compensate for  
441 losses caused by storm erosion. Thus, occurrence time can have significant impacts on  
442 the longevity of nourishment implemented on this beach.

#### 443 **4.3. Implications of nourishment management**

444 Serious beach erosion is observed globally due to the climate change with sea level  
445 rise and more frequent and severe storms (Castelle et al., 2007; Houston and Dean,  
446 2014; Qi et al., 2010; Scott et al., 2016; Smith et al., 2014). Under this circumstance,  
447 there are growing numbers of beach nourishments to meet increasing public  
448 requirements (Kuang et al., 2011). This kind of nourishment coupled with the  
449 consideration of nourishment occurrence time can be an effective way to restore the  
450 beach exposed to frequent storms. Also, placing borrowed sediments should consider  
451 the erosion distribution pattern to achieve better efficiency. Since the nourishment

452 projects were implemented with the same operations and cross-shore position in this  
453 study, we can only suggest that placing the borrowed sediments on the erosion area  
454 alongshore but not the limited easy-access area might cause better efficiency. Many  
455 studies have predicted the evolution of different kinds of sand nourishments by  
456 numerical simulation (Kuang et al., 2011; Pan, 2011), which may make the sand  
457 nourishment more effective. Although the applicability of this work may be limited,  
458 our results can provide a reference for beach management since this kind of  
459 nourishment is common in the local area. Besides, this research can also provide a case  
460 study for protecting eroded beaches around the world, but the implementation on other  
461 beaches needs to consider their respective characteristics and local storm condition.

## 462 **5. Conclusions**

463       Due to the increasing storm erosion of beaches, beach nourishment has become  
464 a wide-used measure. Argus video monitoring system is an effective means to monitor  
465 continuous storm-induced erosion of beaches and corresponding nourishment  
466 effectiveness. In this case study of Dongsha beach, video-derived morphological  
467 parameters of the beach were analyzed over a year, and the following main conclusions  
468 are obtained.

469       Seasonal morphological variation related to storm-intensive period existed on this  
470 beach. Shorelines retreated during autumn and winter when storms were intensive,  
471 while advanced in spring and summer, with a lot of bulges occurred after nourishment  
472 projects. Abrupt variations in the beach orientation were always followed by gradual

473 recoveries to the average, while continuous counter-clockwise rotation occurred after  
474 March, 2017 when storm events were sparse.

475 The implementation of nourishment to prevent storm erosion on embayed beaches  
476 should consider the occurrence time, borrowing sediments timely after the storm event  
477 is the most effective way to compensate for storm erosion in this study. Unsuitable  
478 timing and alongshore position of these nourishments might cause short longevity and  
479 beach rotation. This study can provide a reference for sand nourishments on eroded  
480 beaches, enabling beach management decisions to be implemented reasonably.

481

## 482 **Acknowledgements**

483 This research was funded by the National Key Research and Development Program of  
484 China (No. 2017YFC0405503), the National Natural Science Foundation of China  
485 (NSFC) (No. U1706214). The authors thank Dr. Giorgio Santinelli for his help in data  
486 processing and Google Earth for the open-source remote sensing data. We also thank  
487 the editor and reviewers for their insightful and constructive comments.

## 488 **Declaration of interest**

489 The authors report no conflicts of interest.

## 490 **References**

491 Aarninkhof, S.G.J., Turner, I.L., Dronkers, T.D.T., Caljouw, M., Nipius, L., 200  
492 3. A video-based technique for mapping intertidal beach bathymetry. *Coast.*  
493 *Eng.* 49, 275–289. [https://doi.org/10.1016/S0378-3839\(03\)00064-4](https://doi.org/10.1016/S0378-3839(03)00064-4)  
494 Angnuureng, D.B., Almar, R., Senechal, N., Castelle, B., Addo, K.A., Marieu,  
495 V., Ranasinghe, R., 2017. Shoreline resilience to individual storms and stor

496 m clusters on a meso-macrotidal barred beach. *Geomorphology* 290. <https://doi.org/10.1016/j.geomorph.2017.04.007>

497

498 Archetti, R., Paci, A., Carniel, S., Bonaldo, D., 2016. Optimal index related to  
 499 the shoreline dynamics during a storm: the case of Jesolo beach. *Nat. Haz*  
 500 *ards Earth Syst. Sci.* 16, 1107–1122. [https://doi.org/10.5194/nhess-16-1107-2](https://doi.org/10.5194/nhess-16-1107-2016)  
 501 016

502 Archetti, R., Romagnoli, C., 2011. Analysis of the effects of different storm ev  
 503 ents on shoreline dynamics of an artificially embayed beach. *Earth Surf. P*  
 504 *rocess. Landforms* 36, 1449–1463. <https://doi.org/10.1002/esp.2162>

505 Balouin, Y., Tesson, J., Gervais, M., 2013. Cuspate shoreline relationship with  
 506 nearshore bar dynamics during storm events – field observations at Sete b  
 507 each, France. *J. Coast. Res.* 65, 440–445. <https://doi.org/10.2112/SI65-075.1>

508 Basterretxea, G., Orfila, A., Jordi, A., Fornós, J.J., Tintoré, J., 2007. Evaluation  
 509 of a small volume renourishment strategy on a narrow Mediterranean bea  
 510 ch. *Geomorphology*. <https://doi.org/10.1016/j.geomorph.2006.10.019>

511 Bird, E.C.F., 1985. *Coastline Changes. A Global Review*. John Wiley and Sons,  
 512 Chichester.

513 Boccotti, P. (Ed.), 2000. Chapter 6 The Wave Climate, in: *Wave Mechanics for*  
 514 *Ocean Engineering*. Elsevier, pp. 183–206. [https://doi.org/10.1016/S0422-98](https://doi.org/10.1016/S0422-9894(00)80032-X)  
 515 94(00)80032-X

516 Cai, F., Dean, R.G., Liu, J., 2011. Beach nourishment in China: Status and pro  
 517 spects, in: *Coastal Engineering Proceedings*. p. 31. [https://doi.org/10.9753/ice](https://doi.org/10.9753/ice.v32.management.31)  
 518 [ce.v32.management.31](https://doi.org/10.9753/ice.v32.management.31)

519 Castelle, B., Turner, I.L., Bertin, X., Tomlinson, R., 2009. Beach nourishments  
 520 at Coolangatta Bay over the period 1987–2005: Impacts and lessons. *Coas*  
 521 *t. Eng.* 56, 940–950. <https://doi.org/10.1016/j.coastaleng.2009.05.005>

522 Castelle, B.O., Turner, I.L., Ruessink, B.G., Tomlinson, R.B., 2007. Impact of s  
 523 torms on beach erosion: broad beach (Gold Coast, Australia). *J. Coast. Re*  
 524 *s.* 23, 534–539.

525 Cheng, L., Shi, L., Xia, X., Tong, X., 2014. Sedimentation and recent morphol  
 526 ogical changes at Dongsha beach, Zhujiajian Island , Zhejiang Province. *M*  
 527 *ar. Geol. Quat. Geol.* 34, 37–44.

528 Chiva, L., Pagán, J.I., López, I., Tenza-Abril, A.J., Aragonés, L., Sánchez, I., 2  
 529 018. The effects of sediment used in beach nourishment: Study case El P  
 530 ortet de Moraira beach. *Sci. Total Environ.* 628–629, 64–73. [https://doi.org/](https://doi.org/10.1016/j.scitotenv.2018.02.042)  
 531 [10.1016/j.scitotenv.2018.02.042](https://doi.org/10.1016/j.scitotenv.2018.02.042)

532 Coco, G., Senechal, N., Rejas, A., Bryan, K.R., Capo, S., Parisot, J.P., Brown,

533 J.A., MacMahan, J.H.M., 2014. Beach response to a sequence of extreme  
534 storms. *Geomorphology* 204, 493–501. [https://doi.org/10.1016/j.geomorph.20](https://doi.org/10.1016/j.geomorph.2013.08.028)  
535 13.08.028

536 Cooke, B.C., Jones, A.R., Goodwin, I.D., Bishop, M.J., 2012. Nourishment pra  
537 ctices on Australian sandy beaches: A review. *J. Environ. Manage.* 113, 31  
538 9–327. <https://doi.org/10.1016/j.jenvman.2012.09.025>

539 Dean, R.G., 1983. Principles of beach nourishment, in: *CRC Handbook of Coa*  
540 *stal Processes and Erosion*. CRC Press, pp. 217–232.

541 Dolan, R., Davis, R.E., 1992. An intensity scale for Atlantic coast northeast st  
542 orms. *J. Coast. Res.* 8, 840–853.

543 Duvat, V., Pillet, V., Volto, N., Krien, Y., Cécé, R., Bernard, D., 2019. High h  
544 uman influence on beach response to tropical cyclones in small islands: Sa  
545 int-Martin Island, Lesser Antilles. *Geomorphology* 325, 70–91. [https://doi.or](https://doi.org/10.1016/j.geomorph.2018.09.029)  
546 [g/10.1016/j.geomorph.2018.09.029](https://doi.org/10.1016/j.geomorph.2018.09.029)

547 Elko, N.A., Holman, R.A., Gelfenbaum, G., 2005. Quantifying the Rapid Evolu  
548 tion of a Nourishment Project with Video Imagery. *J. Coast. Res.* 214, 63  
549 3–645. <https://doi.org/10.2112/04-0280.1>

550 Elko, N.A., Wang, P., 2007. Immediate profile and planform evolution of a bea  
551 ch nourishment project with hurricane influences. *Coast. Eng.* 54, 49–66. [h](https://doi.org/10.1016/j.coastaleng.2006.08.001)  
552 [ttps://doi.org/10.1016/j.coastaleng.2006.08.001](https://doi.org/10.1016/j.coastaleng.2006.08.001)

553 Guo, J., Shi, L., Chen, S., Ye, Q., 2019. Response of Dongsha beach in Zhous  
554 han to continuous storms based on Argus images. *Oceanol. Limnol. Sin.* 5  
555 0, 728–739. <https://doi.org/10.11693/hyhz20181200285>

556 Guo, J., Shi, L., Tong, X., Zheng, Y., Xu, D., 2018. The response to tropical  
557 storm Nakri and the restoration of Dongsha Beach in Zhujiajian Island, Zh  
558 ejiang Province. *Haiyang Xuebao* 40, 137–147. [https://doi.org/10.3969/j.iss](https://doi.org/10.3969/j.issn.0253-4193.2018.09.012)  
559 [n.0253-4193.2018.09.012](https://doi.org/10.3969/j.issn.0253-4193.2018.09.012)

560 Hamm, L., Capobianco, M., Dette, H., Lechuga, A., Spanhoff, R., Stive, M.J.,  
561 2002. A summary of European experience with shore nourishment. *Coast.*  
562 *Eng.* 47, 237–264. [https://doi.org/10.1016/S0378-3839\(02\)00127-8](https://doi.org/10.1016/S0378-3839(02)00127-8)

563 Hanson, H., Brampton, A., Capobianco, M., Dette, H., Hamm, L., Lastrup, C.,  
564 Lechuga, A., Spanhoff, R., 2002. Beach nourishment projects, practices, a  
565 nd objectives—a European overview. *Coast. Eng.* 47, 81–111. [https://doi.or](https://doi.org/10.1016/S0378-3839(02)00122-9)  
566 [g/10.1016/S0378-3839\(02\)00122-9](https://doi.org/10.1016/S0378-3839(02)00122-9)

567 Harley, M.D., Andriolo, U., Armaroli, C., Ciavola, P., 2014. Shoreline rotation  
568 and response to nourishment of a gravel embayed beach using a low-cost  
569 video monitoring technique: San Michele-Sassi Neri, Central Italy. *J. Coast.*

570 Conserv. 18, 551–565. <https://doi.org/10.1007/s11852-013-0292-x>

571 Harley, M.D., Turner, I.L., Short, A.D., 2015. New insights into embayed beach  
572 rotation: The importance of wave exposure and cross-shore processes. *J.*  
573 *Geophys. Res. Earth Surf.* 120, 1470–1484. <https://doi.org/10.1002/2014JF00>  
574 3390

575 Houston, J.R., Dean, R.G., 2014. Shoreline Change on the East Coast of Florida  
576 a. *J. Coast. Res.* 30, 647. <https://doi.org/10.2112/JCOASTRES-D-14-00028.1>

577 Hu, R., Wu, J., Li, G., Zhu, L., Ma, F., 2009. Characteristics of sediment transport  
578 in the Zhoushan Archipelago sea area. *Acta Oceanol. Sin.* 28, 116–  
579 27.

580 Kaczkowski, H.L., Kana, T.W., Traynum, S.B., Visser, R., 2018. Beach-fill equilibrium  
581 and dune growth at two large-scale nourishment sites. *Ocean Dyn.*  
582 68, 1191–1206. <https://doi.org/10.1007/s10236-018-1176-2>

583 Karambas, T. V., Samaras, A.G., 2014. Soft shore protection methods: The use  
584 of advanced numerical models in the evaluation of beach nourishment. *Ocean Eng.* 92,  
585 129–136. <https://doi.org/10.1016/j.oceaneng.2014.09.043>

586 Karunaratna, H., Brown, J., Chatzirodou, A., Dissanayake, P., Wisse, P., 2018.  
587 Multi-timescale morphological modelling of a dune-fronted sandy beach. *Coast. Eng.* 136,  
588 161–171. <https://doi.org/10.1016/j.coastaleng.2018.03.005>

589 Karunaratna, H., Pender, D., Ranasinghe, R., Short, A.D., Reeve, D.E., 2014.  
590 The effects of storm clustering on beach profile variability. *Mar. Geol.* 348,  
591 103–112. <https://doi.org/10.1016/j.margeo.2013.12.007>

592 Kuang, C., Mao, X., Gu, J., Niu, H., Ma, Y., Yang, Y., Qiu, R., Zhang, J., 20  
593 19. Morphological processes of two artificial submerged shore-parallel sand  
594 bars for beach nourishment in a nearshore zone. *Ocean Coast. Manag.* 179,  
595 104870. <https://doi.org/10.1016/j.ocecoaman.2019.104870>

596 Kuang, C., Pan, Y., Zhang, Y., Liu, S., Yang, Y., Zhang, J., Dong, P., 2011.  
597 Performance Evaluation of a Beach Nourishment Project at West Beach in  
598 Beidaihe, China. *J. Coast. Res.* 27, 769. <https://doi.org/10.2112/JCOASTRES-D-10-00184.1>

600 Leonard, L., Clayton, T.D., Dixon, K., Pilkey, O.H., 1989. U.S. beach replenishment  
601 experience. A comparison of the Atlantic, Pacific, and Gulf Coasts, in:  
602 Coastal Zone: Proceedings of the Symposium on Coastal and Ocean Management.  
603 pp. 1994–2006.

604 Li, G., Gao, S., Wang, Y., Li, C., 2018. Sediment flux from the Zhoushan Archipelago,  
605 eastern China. *J. Geogr. Sci.* <https://doi.org/10.1007/s11442-018-14>  
606 79-8

607 Liu, G., Cai, F., Qi, H., Zhu, J., Lei, G., Cao, H., Zheng, J., 2019. A method  
608 to nourished beach stability assessment: The case of China. *Ocean Coast.*  
609 *Manag.* 177, 166–178. <https://doi.org/10.1016/j.ocecoaman.2019.05.015>

610 Lu, J., 2010. Research Report on the Regional Climate of 908 Special Island  
611 Survey in Zhejiang Province.

612 Luo, S., Liu, Y., Jin, R., Zhang, J., Wei, W., 2016. A guide to coastal manage  
613 ment: Benefits and lessons learned of beach nourishment practices in Chin  
614 a over the past two decades. *Ocean Coast. Manag.* 134, 207–215. <https://doi.org/10.1016/j.ocecoaman.2016.10.011>

616 Mendoza, E.T., Jimenez, J.A., Mateo, J., 2011. A coastal storms intensity scale  
617 for the Catalan sea (NW Mediterranean). *Nat. Hazards Earth Syst. Sci.* 11,  
618 2453–2462. <https://doi.org/10.5194/nhess-11-2453-2011>

619 Ojeda, E., Guillén, J., 2008. Shoreline dynamics and beach rotation of artificial  
620 embayed beaches. *Mar. Geol.* 253, 51–62. <https://doi.org/10.1016/j.margeo.2008.03.010>

622 Oliveira, S., Moura, D., Horta, J., Nascimento, A., Gomes, A., Veiga-Pires, C.,  
623 2017. The morphosedimentary behaviour of a headland–beach system: Qua  
624 ntifying sediment transport using fluorescent tracers. *Mar. Geol.* 388, 62–7  
625 3. <https://doi.org/10.1016/j.margeo.2017.02.010>

626 Pagán, J.I., López, M., López, I., Tenza-Abril, A.J., Aragonés, L., 2018. Study  
627 of the evolution of gravel beaches nourished with sand. *Sci. Total Environ.*  
628 626, 87–95. <https://doi.org/10.1016/j.scitotenv.2018.01.015>

629 Pan, S., 2011. Modelling beach nourishment under macro-tide conditions. *J. Co  
630 ast. Res.* 64, 2063–2067.

631 Pranzini, E., Anfuso, G., Muñoz-Perez, J.J., 2018. A probabilistic approach to  
632 borrow sediment selection in beach nourishment projects. *Coast. Eng.* 139,  
633 32–35. <https://doi.org/10.1016/j.coastaleng.2018.05.001>

634 Psuty, N.P., Moreira, M.E.S.A., 1992. Characteristics and longevity of beach no  
635 urishment at Praia da Rocha, Portugal. *J. Coast. Res.* 8, 660–676.

636 Qi, H., Cai, F., Lei, G., Cao, H., Shi, F., 2010. The response of three main b  
637 each types to tropical storms in South China. *Mar. Geol.* <https://doi.org/10.1016/j.margeo.2010.06.005>

639 Scott, T., Masselink, G., O’Hare, T., Saulter, A., Poate, T., Russell, P., Davidso  
640 n, M., Conley, D., 2016. The extreme 2013/2014 winter storms: Beach rec  
641 overy along the southwest coast of England. *Mar. Geol.* 382, 224–241. <https://doi.org/10.1016/j.margeo.2016.10.011>

643 Senechal, N., Coco, G., Castelle, B., Marieu, V., 2015. Storm impact on the se

644 asonal shoreline dynamics of a meso- to macrotidal open sandy beach (Bis  
645 carrosse, France). *Geomorphology* 228, 448–461. <https://doi.org/10.1016/j.geomorph.2014.09.025>  
646

647 Seymour, R., Guza, R.T., O'Reilly, W., Elgar, S., 2005. Rapid erosion of a sm  
648 all southern California beach fill. *Coast. Eng.* 52, 151–158. <https://doi.org/10.1016/j.coastaleng.2004.10.003>  
649

650 Short, Andrew D., Masselink, G., 1999. Embayed and structurally controlled be  
651 aches, in: Short, A.D. (Ed.), *Handbook of Beach and Shoreface Morphody  
652 namics*. John Wiley and Sons Ltd., Chichester, pp. 230–250.

653 Smith, A.M.M., Guastella, L.A.A., Botes, Z.A.A., Bundy, S.C.C., Mather, A.A.  
654 A., 2014. Forecasting cyclic coastal erosion on a multi-annual to multi-dec  
655 adal scale: Southeast African coast. *Estuar. Coast. Shelf Sci.* 150, 86–91. <https://doi.org/10.1016/j.ecss.2013.12.010>  
656

657 Stauble, D.K., 2007. Assessing beach fill compatibility through project performa  
658 nce evaluation, in: *Coastal Sediments '07*. American Society of Civil Engi  
659 neers, Reston, VA, pp. 2418–2431. [https://doi.org/10.1061/40926\(239\)190](https://doi.org/10.1061/40926(239)190)

660 Stauble, D.K., 1988. Beach nourishment monitoring, a necessity to project desi  
661 gn. *Beach Preserv. Technol.* 88 Probl. Adv. Beach Nourishment 88, 87–98.

662 Third Institute of Oceanography, 2010. *Coast erosion assessment and control: T  
663 he final investigation and assessment*.

664 Wiggins, M., Scott, T., Masselink, G., Russell, P., McCarroll, R.J., 2019. Coast  
665 al embayment rotation: Response to extreme events and climate control, us  
666 ing full embayment surveys. *Geomorphology*. <https://doi.org/10.1016/j.geomorph.2018.11.014>  
667

668 Xia, X., 2014. *China's Islands: Zhejiang (Volume II: Zhoushan Archipelago)*. C  
669 hina Ocean Press, Beijing.